JOC The Journal of Organic Chemistry

Article

pubs.acs.org/joc

1,4-Naphthalenediyl-Bridged Molecular Gyrotops: Rotation of the Rotor and Fluorescence in Solution

Yohei Nishiyama,[†] Yusuke Inagaki,[†] Kentaro Yamaguchi,[‡] and Wataru Setaka*[,†]

[†]Division of Applied Chemistry, Faculty of Urban Environmental Sciences, Tokyo Metropolitan University, Hachioji, Tokyo 192-0397, Japan

[‡]Faculty of Pharmaceutical Sciences at Kagawa Campus, Tokushima Bunri University, Sanuki, Kagawa 769-2193, Japan

Supporting Information

ABSTRACT: Macrocage molecules with a bridged π-electron system have been reported as molecular gyrotops in which the π-electron system can rotate within the cage. We recently reported the dynamics of the rotor in solution using 1,4-naphthalenediyl-bridged molecular gyrotops, which consist of cages formed of three C_{14}, C_{16}, or C_{18} chains. In this work, we synthesized novel gyrotops with C_{15} and C_{17} chains and systematically investigated the activation energies for the rotation of the rotor in solution. The activation energies for rotation in solution were found to decrease with increasing size of the cage. Therefore, a rotational barrier can be designed by adjusting the length of the side chains in these molecular gyrotops. Additionally, these gyrotops were fluorescent in solution; the quantum yields and lifetimes of the fluorescence were investigated. However, these properties were not influenced by the chain length owing to a large difference in time scale between fluorescence (10^{-8}–10^{-9} s) and the rotational dynamics inside the cage (10^{0}–10^{-5} s).

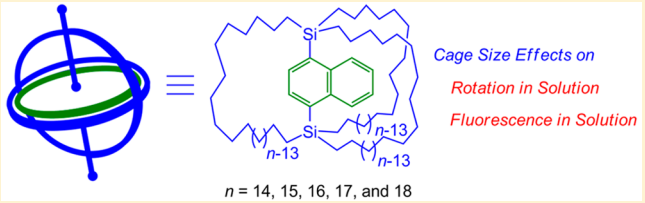

INTRODUCTION

Artificial molecular rotors that show rotation of a part of the molecule have recently become a widely investigated topic because the molecular motion could affect the properties and reactivity of these molecules. The chemical field of artificial molecular machines aims to design novel molecular-based materials in which these motions are controlled.[1−7] For this reason, macrocage molecules with a bridged π-electron system have been reported as molecular gyroscopes and gyrotops because the π-electron system can rotate rapidly inside a cage framework.[2−5] The synthesis, structure, and dynamics of molecular gyroscopes and gyrotops have been investigated by Garcia-Garibay et al.,[2,6] Gladysz et al.,[3] and our group.[4,5]

We synthesized a crystalline molecular gyrotop **1** with a phenylene rotor and showed the rotation of the rotor inside a cage, accompanied by a thermal change in the birefringence of the single crystal.[4e] The effects of the chain length (C_{14}, C_{16}, and C_{18} chains) on the dynamic properties of the molecular gyrotops in a crystalline state have recently been reported.[4a] Phenylene is suitable for the gyrotop rotor in a crystalline state because it is a symmetric and small π-electron system. However, it is difficult to investigate the dynamics of the rotor in solution due to the axial symmetry of the rotor.

We recently reported the synthesis and structure of 1,4-naphthalenediyl-bridged molecular gyrotops (**C14**, **C16**, and **C18** in Figure 1) and revealed the chain length (C_{14}, C_{16}, and C_{18} chains) dependence of the rotation of the rotor in solution.[4d] As the 1,4-naphthalenediyl rotor is axially asymmetric, slow rotation of the rotor inside the cage, at less than the NMR time scale, can be easily observed as asymmetric NMR signals from the cage framework. In contrast, rapid rotation of the rotor is confirmed by symmetric NMR signals from the cage due to chemical exchange within the asymmetric structure.

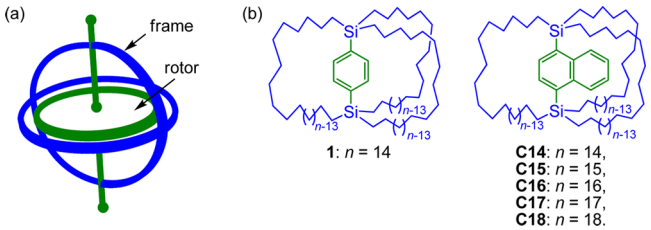

Figure 1. (a) A model gyrotop. (b) Structural formula of molecular gyrotops **1** and **C14**–**C18**.

In this report, novel molecular gyrotops (**C15** and **C17** in Figure 1) with medium alkyl chains (C_{15} and C_{17} chains) forming the cages were designed and synthesized. Synthesis of the cage revealed that the yield had a remarkable chain length dependence. The activation energies for rotation of the rotor were estimated by investigating the temperature dependence of the line shape of the ^{13}C NMR signal and ^{13}C–^{13}C exchange spectroscopy (EXSY) NMR.[8,9] Thus, the effects of cage size on the barrier to rotation of the naphthalenediyl rotor were revealed systematically and accurately. Additionally, the fluorescence properties, such as the quantum yields and lifetimes, of these gyrotops in solution were investigated.

Received: July 1, 2015
Published: September 16, 2015

DOI: 10.1021/acs.joc.5b01489
J. Org. Chem. 2015, 80, 9959−9966

Scheme 1. Synthesis of Molecular Gyrotops (C14−C18) and Noncage Isomers (C14i−C18i) with a 1,4-Naphthalenediyl Rotor

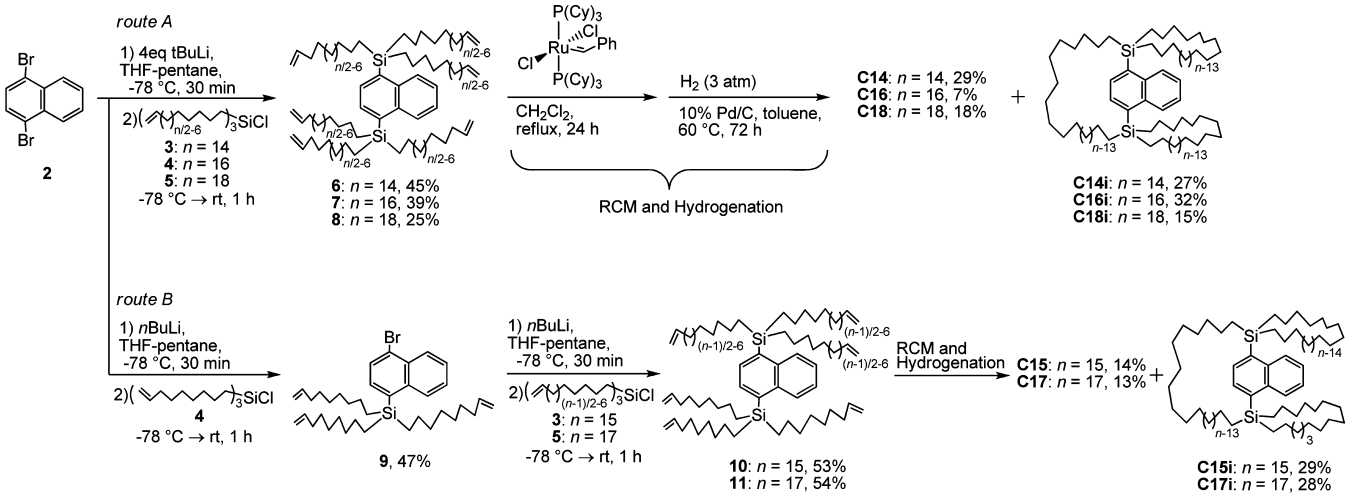

However, these properties were found to be unaffected by the chain length owing to a large difference in time scale between fluorescence and the rotational dynamics inside the cage. The basic studies of the properties of these simple caged compounds will allow implementation of novel principles for the molecular design of new functional molecules. For this reason, a series of cage-like cyclophanes containing a fluorophore were synthesized, and their basic characteristics as functional molecules were investigated.

RESULTS AND DISCUSSION

Synthesis of Molecular Gyrotops. Synthesis of 1,4-naphthalenediyl-bridged molecular gyrotops (**C14**, **C16**, and **C18**) with even-numbered alkyl chain lengths (C_{14}, C_{16}, and C_{18} chains) forming the cage was previously reported (Scheme 1, route A).[4d] They were synthesized by ring-closing metathesis[10] (RCM) reaction of bissilylnaphthalene (**6**−**8**) and subsequent hydrogenation of the unsaturated cage. The cages were separated from the mixture by preparative gel permeation chromatography (GPC). The structural identification of the cages was reported in the previous report.[4d] The structure of **C14i** was identified from ^{13}C NMR spectra. Owing to the structural symmetry of **C14i**, 14 methylene signals were observed, half of which had signal intensities twice as large as the other half. The ^{13}C NMR spectra of **C16i** and **C18i** showed similar signal patterns, although some of the signals were overlapped. As these isomers (**C14i**, **C16i**, and **C18i**) were obtained as oils, structural analysis by X-ray crystallography could not be carried out. For reference, the crystal structures of the phenylene derivatives of **C18i** were reported previously.[4b]

To synthesize molecular gyrotops with odd-numbered alkyl chain lengths (**C15** and **C17**), introduction of different trialkenylsilyl groups to naphthalene is necessary. Therefore, stepwise silylations of naphthalene were performed (Scheme 1, route B). Monolithiation of 1,4-dibromonaphthalene with *n*-BuLi, followed by a substitution reaction with tri(8-nonenyl)-chlorosilane (**4**), afforded 1-bromo-4-silylnaphthalene **9** in a 47% yield. Bissilylnaphthalenes (**10** and **11**) were obtained from **9** in 53% and 54% yields, respectively, via similar lithiation and substitution reactions. The RCM reaction of **10** and **11** in the presence of Grubbs' first-generation catalyst, followed by hydrogenation of the unsaturated cage, gave the corresponding desired cages [**C15** (14% yield) and **C17** (13% yield)] along with the formation of structural isomers [**C15i** (29% yield) and **C17i** (28% yield)]. The cages and isomers were separated by preparative gel permeation chromatography (GPC). The structures of the cages were identified by NMR spectroscopy and single-crystal X-ray diffraction studies, as described later. The structural identification of the isomers (**C15i** and **C17i**) was difficult because the NMR signals of the methylenes were intricately overlapped owing to the different lengths of the two methylene chains adjacent to the same silicon in **C15i** (C_{14} and C_{16} chains) and **C17i** (C_{16} and C_{18} chains). Hence, the structures were assigned using the MS spectra and in comparison with the NMR spectra of **C14i**.

The product ratios and yields of the cages are summarized in Table 1. A remarkable chain length dependence of the product ratios in the RCM reaction of bissilylnaphthalenes was observed. The cage/isomer product ratios are larger than the statistic ratios in the synthesis of **C14**, **C15**, **C17**, and **C18**; this is because the statistical ratio of formation of the cage and the isomer, derived from probability theory, in this RCM reaction was cage/isomer = 1/3.[4b] The reason for the predominant formation of the isomer in the synthesis of **C16** remains unclear. It is possible that the odd length of the alkenyl chains (C_9 chains) in the precursor may prevent formation of the cage. A similar chain length dependence of the cage/isomer product ratio was observed in the synthesis of the phenylene-bridged derivatives.[4a]

Table 1. Yields of the Cages and Their Isomers in RCM Reactions of Bissilylnaphthalenes (6, 7, 8, 10, and 11)

	yield (%)		ratio[a]
precursor	cage	isomer	cage:isomer
6 (n = 14)[b]	29	27	5:5
10 (n = 15)	14	29	3:7
7 (n = 16)[b]	7	32	2:9
11 (n = 17)	13	28	3:7
8 (n = 18)[b]	18	15	5:5

[a]Product ratio. [b]Reference 4d.

Molecular Structure Determined by Single-Crystal X-ray Diffraction Studies. Single-crystal X-ray diffraction studies were performed to determine the molecular structure of the crystalline state. Recrystallization to obtain a single

DOI: 10.1021/acs.joc.5b01489
J. Org. Chem. 2015, 80, 9959−9966

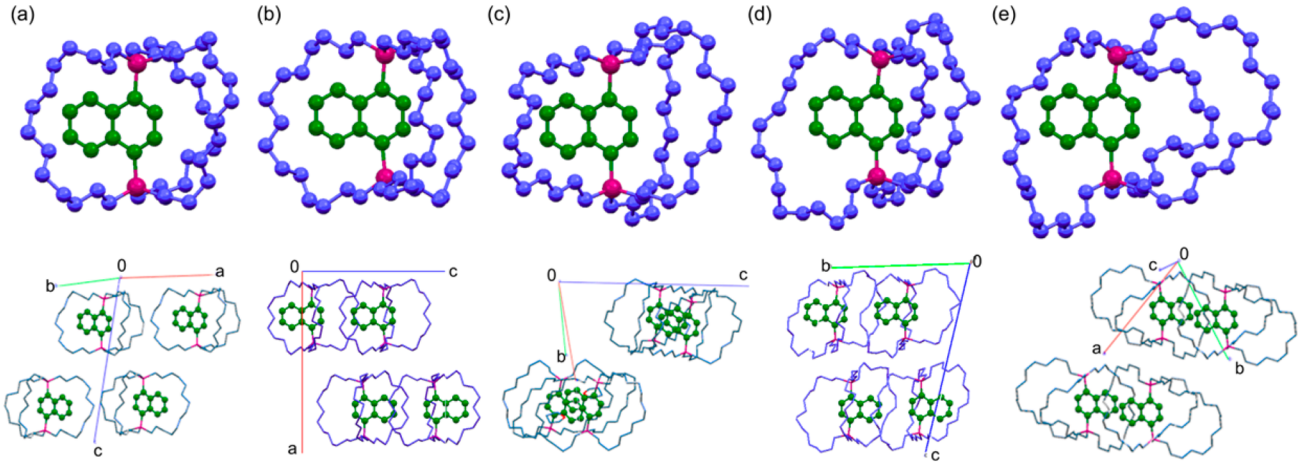

Figure 2. Molecular structures of molecular gyrotops **C14**–**C18** as determined by X-ray crystallography (ball-and-stick model). Hydrogen atoms are omitted for clarity. Molecular structure (top row) and crystal structure (bottom row): (a) **C14**,[4d] (b) **C15**, (c) **C16**,[4d] (d) **C17**, (e) **C18**.[4d]

crystal of the cages (**C14**–**C18**) was conducted by evaporation from a tetrahydrofuran (THF)/methanol (4:1 v/v) solution. Unfortunately, the isomers (**C14i**–**C18i**) were not crystallized owing to their oily nature. We previously reported the molecular structures of **C14**, **C16**, and **C18** as determined by X-ray crystallography.[4d] In this study, the structures of **C15** and **C17** were analyzed; however, the structures were not refined well (i.e., final *R* indices of greater than 10%), because of the following undesirable characteristics. A rotational twin existed in the single crystal of **C15**, of which the crystal system and space group are monoclinic and $P2_1/c$, respectively, because the β angle of the unit cell is close to 90°. For **C17**, intense reflection data could not be collected even at low temperature (90 K) because the single crystals were too thin.

The molecular structures of molecular gyrotops **C14**–**C18** as determined by X-ray crystallography are shown in Figure 2. In all the compounds, the bissilylnaphthalene moiety was effectively surrounded by three alkyl chains. Comparing the molecular structures among molecular gyrotops **C14**–**C18**, we observed that the shape of the cage was deformed from the spherical shape in the compounds containing long alkyl chains (e.g., **C18**). The calculated densities of the crystals decreased with expansion of the cage size: 1.047 g/cm^3 for **C14**, 1.040 g/cm^3 for **C15**, 1.026 g/cm^3 for **C16** [solvent molecules (THF) were included in this crystal], 1.027 g/cm^3 for **C17** [the observed temperature (90 K) differed from the others (120 K)], and 1.019 g/cm^3 for **C18**, most likely because the void spaces between the cage and the rotor increased with increasing cage size.

All of the crystal structures of the molecular gyrotops (**C14**–**C18**) have similar features, such that the molecules could be stacked along their rotation axes. As described in the previous report, π-stacked aggregates of molecules were formed in the crystal structure of **C16** and **C18**.[4d] However, the other molecules (**C14**, **C15**, and **C17**) existed as a single molecule in the crystal. The melting points of the present molecules (**C14**–**C18**) were nearly identical, although their crystal structures differ slightly.

Rotation of a 1,4-Naphthalenediyl Rotor in Solution. The rotation of the 1,4-naphthalenediyl rotor of the molecular gyrotops in solution was investigated by temperature-dependent NMR spectroscopy. Although chemically inequivalent methylene signals of the molecular gyrotops overlapped in the ^{1}H NMR spectra (see the Supporting Information), the corresponding methylene signals of the ^{13}C NMR spectra were well-resolved (Figure 3). Hence, the rotation of the rotor was

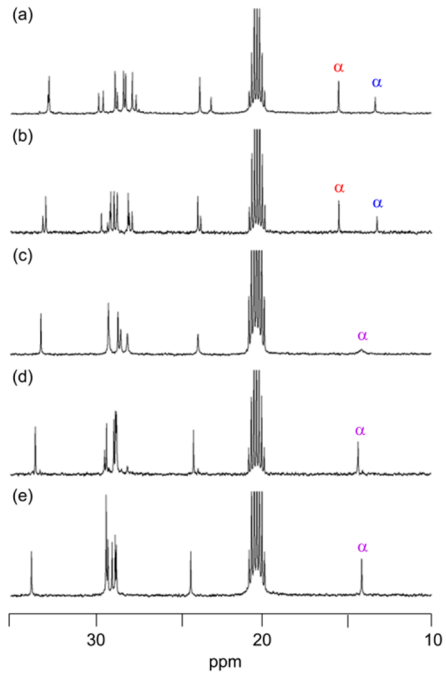

Figure 3. ^{13}C NMR spectra (125 MHz) of compounds (a) **C14**,[4d] (b) **C15**, (c) **C16**,[4d] (d) **C17**, and (e) **C18**[4d] in toluene-d_8 at 300 K (methylene region). The signals of methylene carbons adjacent to silicon atoms are indicated by the symbol α.

studied using ^{13}C NMR spectroscopy. The alkyl region (10–35 ppm) of the ^{13}C NMR spectra of the molecular gyrotops, recorded at 300 K in toluene-d_8, is shown in Figure 3. The signals of methylenes adjacent to silicon, which are indicated by the symbol α in Figure 3, were assigned by analyses of the ^{1}H–^{13}C HSQC and ^{1}H–^{13}C HMBC NMR spectra. For instance, the signal assignments in **C15** were carried out as follows: In the HSQC spectrum (Figure S18), the carbons corresponding to the signals at 13.0 and 15.3 ppm are connected to the protons corresponding to the signals at 1.03 and 1.09 + 0.79 (magnetically inequivalent protons) ppm, respectively. In the HMBC spectrum (Figure S19), only these

DOI: 10.1021/acs.joc.5b01489
J. Org. Chem. 2015, 80, 9959–9966

methylene protons show cross-peaks with the naphthalene carbons connected to silicon (δ 136.9). These observations indicate that the methylenes corresponding to the signals at 13.0 and 15.3 ppm are located closest to the naphthalene ring.

In the ^{13}C NMR spectrum of **C14** (Figure 3, a), 14 methylene signals were observed, half of which had twice the intensity of the other half.[4d] This indicates that two of the three alkyl chains are identical on the time scale of the NMR experiment and that the cage of **C14** possesses *quasi*-C_{2v} symmetry. Hence, the rotation of the naphthalene ring is very slow, or stopped, inside the cage. In the ^{13}C NMR spectrum of **C15** (Figure 3, b), the observed spectral features were identical to those of **C14**, indicating slow dynamics of the rotor. In the spectrum of **C16** (Figure 3, c), the methylene signals were broadened owing to the restricted rotation of the rotor.[4d] In the spectrum of **C18** (Figure 3, e), nine methylene signals were observed, indicating that the three alkyl chains were identical on the NMR time scale owing to rapid rotation of the internal naphthalenediyl rotor inside the cage, as shown in a previous report.[4d] Similar spectral features were observed in the spectrum of **C17** (Figure 3, d), indicating rapid rotation of the rotor.

To estimate the energy barrier for the rotation of the rotor, temperature-dependent ^{13}C NMR spectra were investigated. As described in the previous report, ^{13}C NMR spectra of **C16** in toluene-d_8 showed a remarkable temperature dependence of the line shapes of the methylene signals.[4d] Simulation of the spectral line shapes assuming a three-site exchange model (Figure 4) allowed estimation of the exchange rate constants

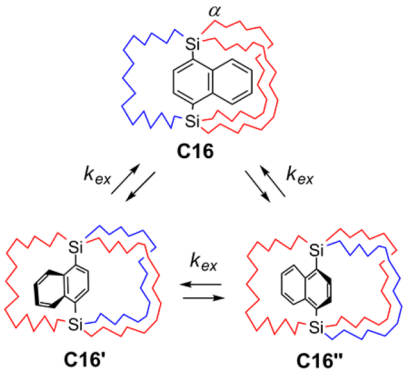

Figure 4. Schematic representation of the three-site exchange model of the dynamics of the molecular gyrotop **C16**.

(k_{ex}) at each observed temperature. The thermodynamic parameters for the exchange for **C16** were estimated to be $\Delta H^{\ddagger}$ = 9.42 ± 0.08 kcal mol^{-1} and $\Delta S^{\ddagger}$ = −12.0 ± 0.3 cal mol^{-1} K^{-1} by using an Eyring plot.[4d]

Temperature-dependent ^{13}C NMR spectra of **C17** in toluene-d_8 were investigated (Figure 5). The line shapes of the methylene signals exhibited a remarkable temperature dependence. An inverse gate pulse sequence was used for the experiments to suppress the nuclear Overhauser effect in the spectra. Two signals at 12.2 and 15.1 ppm assignable to methylenes adjacent to silicon atoms, i.e., α-methylenes in Figure 3d, at 210 K showed remarkable temperature dependence. With increasing temperature, these signals broadened and coalesced at around 230 K and became a sharp singlet above ambient temperature. The exchange rate constants (k_{ex}) at each temperature were estimated by line shape analysis assuming the three-site exchange model shown in Figure 4. The activation

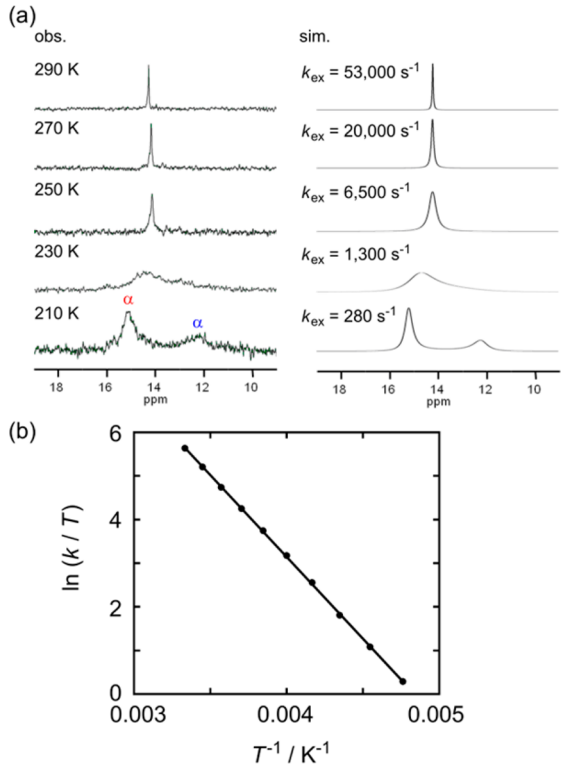

Figure 5. (a) Temperature-dependent ^{13}C NMR spectra of **C17** in toluene-d_8 (α-methylene). Left: observed spectra. Right: simulated spectra with designated exchange rate constants (k_{ex}). (b) Eyring plot for naphthalenediyl rotation in **C17**. The k_{ex} values are determined from temperature-dependent ^{13}C NMR spectroscopy.

enthalpy and entropy for the rotation of the rotor in **C17** were estimated to be $\Delta H^{\ddagger}$ = 7.49 ± 0.26 kcal mol^{-1} and $\Delta S^{\ddagger}$ = −11.0 ± 1.0 cal mol^{-1} K^{-1}, respectively, from the linear plot of $\ln(k_{ex}/T)$ versus $1/T$ (Eyring plot, Figure 5b).

The temperature dependence of the ^{13}C NMR spectra (1D-complete) of **C15** was also investigated; however, the line shapes of the methylene signals remained unchanged. Hence, the very slow chemical exchange processes in **C15** were investigated by $^{13}C-^{13}C$ EXSY NMR. EXSY NMR is useful for analysis of slow chemical exchanges, which are observed as intensity differences between exchangeable signals of cross-peaks and diagonal peaks.[8,9] Figure 6a shows the temperature-dependent $^{13}C-^{13}C$ EXSY NMR spectra of **C15** in toluene-d_8 with a mixing time of 400 ms. Cross-peaks between exchangeable methylene protons adjacent to silicon atoms, i.e., α-methylenes in Figure 3b, were observed, and the intensities of the signals were remarkably temperature-dependent. Although the exchange process is strictly represented by a three-site exchange mechanism (Figure 4), it reduces to a two-site exchange (eq 1), as two of the three structures were indistinguishable. Figure 6 also shows the rate constants (k_{ex}) for the chemical exchange (eq 1). The estimated exchange constants, which are comparable to the exchange rates for the three-site exchange model (Figure 4), can be estimated by analyzing the signal intensities of the cross-peaks and diagonal peaks using the EXSY Calc software.[11] The activation enthalpy ($\Delta H^{\ddagger}$) and entropy ($\Delta S^{\ddagger}$) for the rotation of the rotor in **C15** were estimated to be 14.6 ± 2.78 kcal mol^{-1} and −11.9 ± 8.7 cal mol^{-1} K^{-1}, respectively, from the Eyring plot (Figure 6b).

DOI: 10.1021/acs.joc.5b01489
J. Org. Chem. 2015, 80, 9959−9966

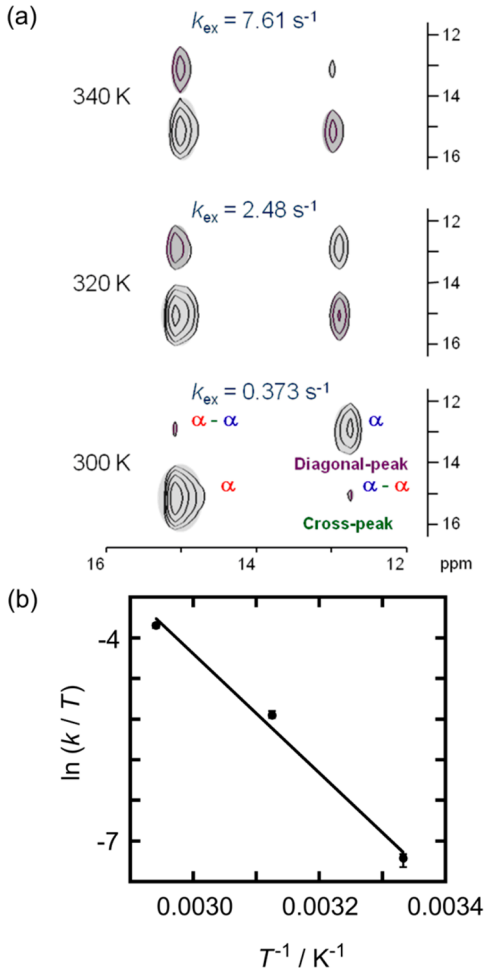

Figure 6. Temperature-dependent $^{13}C-^{13}C$ EXSY NMR spectra of **C15** in toluene-d_8 (α-methylenes) with a mixing time of 400 ms. Exchange rate constants (k_{ex}) estimated by EXSY Calc software are also indicated. (b) Eyring plot for naphthalenediyl rotation in **C15**.

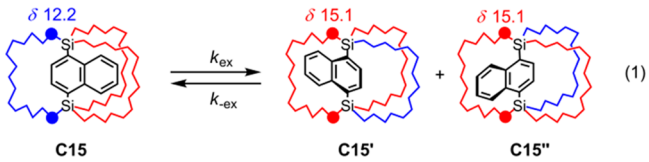

The dynamics of the naphthalenediyl rotor in **C14** is expected to be slower than that of **C15**. Therefore, the $^{13}C-^{13}C$ EXSY NMR spectrum of **C14** was also investigated. However, no cross-peaks between exchangeable methylene protons were observed (Figure S44). Hence, the dynamics is considered to stop or be much slower than the NMR time scale.

Unfortunately, the energy barriers for the rotation of the rotor of **C14** and **C18** could not be estimated. The temperature dependence of the ^{13}C NMR spectra of **C14** and **C18** were reinvestigated, and the results are shown in Figures S41 and S42 and Table S2 in the Supporting Information. The chemical shifts of the signals were slightly changed by varying the temperature, indicating that the equilibrium cage structures were temperature-dependent. However, the details of the structural change were not apparent. The signal line widths of the methylene signals, as well as the aromatic signals, were broadened with decreasing temperature. The line broadening is not ascribed to rotational dynamics of the rotor, but to the increasing viscosity of the solvent.

The estimated activation enthalpies ($\Delta H^{\ddagger}$) and entropies ($\Delta S^{\ddagger}$) for the rotation of the 1,4-naphthalenediyl rotor in the molecular gyrotops are summarized in Table 2. It is apparent

Table 2. Thermodynamic Parameters for Rotor Rotation in Molecular Gyrotops C14−C18

	rotation parameters[b]		
gyrotop	$\Delta H^{\ddagger}$/kcal mol^{-1}	$\Delta S^{\ddagger}$/cal mol^{-1} K^{-1}	k_{ex}/s^{-1} at 300 K
C14[a]	>14.6[c]	[c]	<0.37
C15	14.6 ± 2.78	−11.9 ± 8.7	0.37
C16[a]	9.42 ± 0.08	−12.0 ± 0.3	2200
C17	7.46 ± 0.10	−11.2 ± 0.4	60 000
C18[a]	<7.46[c]	[c]	>60 000

[a]Reference 4d. [b]The errors are standard deviations. [c]The parameter could not be determined uniquely.

that the activation enthalpies for rotation in the molecular gyrotops (14.6 ± 2.78 kcal mol^{-1} for **C15**, 9.42 ± 0.08 kcal mol^{-1} for **C16**, and 7.46 ± 0.10 kcal mol^{-1} for **C17**) decreased with increasing length of the alkyl side chains of the cage. The large negative $\Delta S^{\ddagger}$ values (−11.9 ± 8.7 cal mol^{-1} K^{-1} for **C15**, −12.0 ± 0.3 cal mol^{-1} K^{-1} for **C16**, and −11.2 ± 0.4 cal mol^{-1} K^{-1} for **C17**) for rotation of the naphthalene ring inside the cage indicate a tight dynamic transition state.

Fluorescence Properties of the Cage and Noncage Isomers in Solution. Naphthalene is known as one of the fluorophores having π-electron systems. The fluorescence properties of silylnaphthalenes in solution have been reported so far.[12] In this study, the effects of the cage on the fluorescence properties, i.e., the quantum yield and florescence lifetime, of 1,4-bissilylnaphthalenes were investigated using the molecular gyrotops (**C14−C18**) and their isomers (**C14i−C18i**).

Figure 7 shows absorption spectra of a hexane solution of bissilylnaphthalenes between 230 and 360 nm. An intense

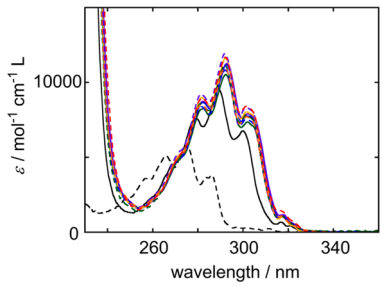

Figure 7. Absorption spectra of 1,4-bissilylnaphthalenes in *n*-hexane (230−360 nm) [**np** (black broken), **TMSnp** (black solid), **C14** (purple solid), **C14i** (purple broken), **C15** (blue solid), **C15i** (blue broken), **C16** (green solid), **C16i** (green broken), **C17** (orange solid), **C17i** (orange broken), **C18** (red solid), **C18i** (red broken)].

absorption band around 290 nm with vibronic structures is assignable to Platt's L_a band, and a weak band at 317 nm is assignable to the L_b band. The absorption bands of caged naphthalenes (**C14−C18**) and their isomers (**C14i−C18i**) were slightly red-shifted compared with those of 1,4-bis(trimethylsilyl)naphthalene (**TMSnp**).

Figure 8 shows the fluorescence spectra of the bissilylnaphthalenes in degassed hexane irradiated at 265 nm. Fluorescence bands with vibronic structures from localized excited states were observed. The fluorescence band maxima for all the bissilylnaphthalenes were 332 nm. The fluorescence quantum

DOI: 10.1021/acs.joc.5b01489
J. Org. Chem. 2015, 80, 9959−9966

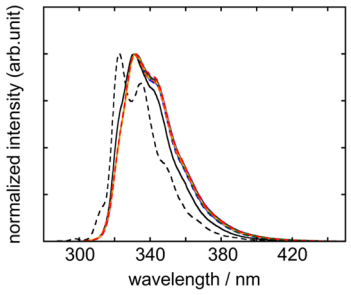

Figure 8. Fluorescence spectra of 1,4-bissilylnaphthalenes in *n*-hexane (degassed 1.0×10^{-6} M solution, irradiated at 265 nm) [**np** (black broken), **TMSnp** (black solid), **C14** (purple solid), **C14i** (purple broken), **C15** (blue solid), **C15i** (blue broken), **C16** (green solid), **C16i** (green broken), **C17** (orange solid), **C17i** (orange broken), **C18** (red solid), **C18i** (red broken)].

yields (Φ) and fluorescence lifetimes (τ_0) of the bissilylnaphthalenes in hexane solution (10 μM) were also investigated. To suppress fluorescence quenching by oxygen completely, the samples were degassed by a freeze–pump–thaw method before the measurements. The results are summarized in Table 3. The

Table 3. Fluorescence Parameters of Bissilylnaphthalenes C14–C18

compound	λ_{max}[a]/nm	Φ[b]	τ_0[d]/ns
np	323	0.10[c]	115.6 ± 8.5
TMSnp	331	0.11	36.7 ± 2.2
C14	332	0.12	23.5 ± 2.2
C14i	332	0.11	26.5 ± 2.4
C15	332	0.12	23.3 ± 2.2
C15i	332	0.12	27.0 ± 2.0
C16	332	0.10	26.7 ± 2.3
C16i	332	0.12	27.0 ± 2.1
C17	332	0.10	25.1 ± 2.0
C17i	332	0.11	26.3 ± 2.3
C18	332	0.11	26.1 ± 2.7
C18i	332	0.11	26.1 ± 2.0

[a]Quantum yields were determined by comparing fluorescence intensity of naphthalene in hexane (Φ = 0.10, ref 13) under irradiation by 262 nm light. [b]Reference 13. [c]Lifetimes were measured under irradiation by 280 nm light with a time-correlated single-photon counting apparatus.

quantum yields of the cages (**C14–C18**) and the isomers (**C14i–C18i**) were almost identical within a range of 0.10–0.12, and the fluorescence lifetimes of the cages and isomers were also identical within a range of 23.5–27.0 ns. The results indicate that the fluorescence properties, such as the band maxima, quantum yields, and lifetimes, of the cage and noncage isomers showed no dependence on the side chain length. Because the time scale of the fluorescence (10^{-8}–10^{-9} s) is much faster than that of the dynamics of the naphthalene rotor (10°–10^{-5} s), as described above, these fluorescence properties of the caged naphthalenes were not influenced by the dynamics of the naphthalenediyl rotors inside the cage.

CONCLUSIONS

We systematically investigated the chain length (C_{14}, C_{15}, C_{16}, C_{17}, and C_{18} chains) dependence of the rotation of the rotor in solution using 1,4-naphthalenediyl-bridged molecular gyrotops. Specifically, molecular gyrotops with odd-length alkyl chains (**C15** and **C17**) were synthesized by stepwise introduction of different trialkenylsilanes into naphthalene, followed by RCM and hydrogenation reactions. The structures of the molecular gyrotops were confirmed by X-ray crystallography, and the calculated densities of the crystals were found to decrease with increasing cage size, most likely owing to expansion of the void spaces inside the cage. The rotation of the naphthalenediyl rotor inside the cage in solution was investigated by temperature-dependent ^{13}C NMR spectroscopy. The activation energies for the rotation in solution were found to decrease with increasing cage size. The fluorescence properties, such as the band maxima, quantum yields, and fluorescence lifetimes, of the cages as well as the noncage isomers were also investigated. However, these properties were not influenced by the side chain length because the time scale of the fluorescence (10^{-8}–10^{-9} s) is much faster than that of the dynamics of the naphthalene rotor (10°–10^{-5} s). Although it is considerable that collision between the alkyl chains consisted of the cage and the naphthalene fluorophore quenches the fluorescence of the naphthalene, the quantum yields of the fluorescence in gyrotops were not depend on the size of the chains. The observation of no cage dependence on the fluorescence properties of these molecules is important for their development as functional molecules.

EXPERIMENTAL SECTION

General. All reactions were conducted under an argon atmosphere. The chemical shifts of ^{1}H and ^{13}C NMR spectra are based on the residual solvent resonances, except for ^{29}Si NMR, in which the chemical shifts were referenced to external tetramethylsilane. ^{13}C–^{13}C EXSY NMR spectra were recorded using a NOESY pulse sequence with a mixing time of 400 ms and initial delay of 8 s. HRMS analyses were carried out by electrospray ionization (ESI) using an FT-ICR-MS system. The sample solutions for HRMS were prepared in a mixture of chloroform/methanol with a small amount of NaI. Preparatory GPC was carried out using a recycling preparative chromatograph; chloroform stabilized with ethanol was used as the eluent. Fluorescence spectra were obtained for samples that were degassed by argon bubbling before the measurements. Fluorescence quantum yields, lifetime measurements, and quenching experiments were carried out with samples thoroughly degassed by several freeze–pump–thaw sequences.

Materials. Commercially available reagents were used without further purification. Grubbs' first-generation catalyst, which is commercially available, was used for all the RCM reactions because, under reflux in dichloromethane, this catalyst was determined to be optimal for the synthesis of the phenylene-bridged derivatives previously reported in ref 4b. Trialkenylchlorosilanes (**3**, **4**, and **5**), bissilylnaphthalenes (**6**, **7**, and **8**), and molecular gyrotops (**C14**, **C16**, and **C18**) were synthesized according to literature procedures.[4]

Synthesis of 1-Bromo-4-(tri-8-nonenylsilyl)naphthalene (9). *p*-Dibromonaphthalene (1.00 g, 3.50 mmol) and dry diethylether (90 mL) were placed in a Schlenk flask (200 mL). *n*-BuLi solution (1.6 M in hexane, 2.0 mL, 1.0 equiv) was added dropwise to the flask at −78 °C. The reaction mixture turned yellow and was stirred for an additional 30 min, after which tri-8-nonenylchlorosilane (**4**, 2.00 g, 4.55 mmol) was added at −78 °C. The reaction mixture was warmed to room temperature for 1 h, and after stirring for 12 h, the mixture was hydrolyzed with dilute HCl (aq) solution and extracted with hexane. The organic layer was washed with saturated $NaHCO_3$ (aq) solution and dried over anhydrous Na_2SO_4. Silica gel column chromatography of the concentrated residue afforded **9** as a colorless oil (0.90 g, 1.47 mmol, 47% yield). **9**: ^{1}H NMR ($CDCl_3$, 500 MHz) δ 0.95–1.08 (m, 6H), 1.20–1.45 (m, 30H), 2.04 (q, J = 6.7 Hz, 6H), 4.95 (d, J = 10.0, 3H), 5.01 (d, J = 17.0 Hz, 3H), 5.81 (ddt, J = 17.0, 10.0, 6.7 Hz), 7.49 (d, J = 7.25 Hz, 1H), 7.56 (t, J = 8.5 Hz, 1H), 7.60 (t, J = 8.5 Hz, 1H), 7.77 (d, J = 7.25 Hz, 1H), 8.12 (d, J = 8.5 Hz, 1H),

DOI: 10.1021/acs.joc.5b01489
J. Org. Chem. 2015, 80, 9959–9966

8.35 (d, J = 8.5 Hz, 1H); ^{13}C NMR ($CDCl_3$, 125 MHz) δ 13.5 (1C), 24.0 (1C), 29.0 (1C), 29.1(2C), 33.6 (1C), 33.9 (1C), 114.2 (1C), 125.6 (1C), 126.4 (1C), 126.7 (1C), 128.2 (1C), 128.3 (1C), 129.4 (1C), 131.9 (1C), 134.4 (1C), 136.5 (1C), 138.8 (1C), 139.2 (1C); ^{29}Si NMR ($CDCl_3$, 99.4 MHz) δ −0.4; HRMS (ESI positive) m/z calcd for $C_{37}H_{57}BrSi$ + Na^+: 631.33051, found: 631.33055.

Synthesis of 1-(Tri-7-octenylsilyl)-4-(tri-8-nonenylsilyl)-naphthalene (10). Bissilylnaphthalene **10** was synthesized by the same procedure as **9**, i.e., lithiation and silylation. In this case, the following reagents were used: 1-bromo-4-(tri-8-nonenylsilyl)-naphthalene (**9**, 1.74 g, 2.86 mmol), THF (15 mL), n-BuLi solution (1.6 M in hexane, 2 mL, 1.0 equiv), and tri-7-octenylchlorosilane (**3**, 1.34 g, 3.37 mmol). Pure compound **10** (1.36 g, 1.52 mmol) was obtained as a colorless oil in 53% yield after GPC purification of the crude products. **10**: a colorless oil; ^{1}H NMR ($CDCl_3$, 500 MHz) δ 0.91−1.08 (m, 12H), 1.15−1.45 (m, 54H), 2.01 (q, J = 7.1 Hz, 12H), 4.90−4.95 (m, 6H), 4.95−5.02 (m, 6H), 5.79 (ddt, J = 17.0, 10.0, 6.5 Hz, 3H), 5.80 (ddt, J = 17.0, 10.0, 6.5 Hz, 3H), 7.47 (dd, J = 6.3, 3.3 Hz, 2H), 7.60 (s, 2H), 8.11 (dd, J = 6.3, 3.3 Hz, 2H); ^{13}C NMR ($CDCl_3$, 125 MHz) δ 13.6 (1C), 24.0 (2C), 28.7 (1C), 29.0 (4C), 29.1 (1C), 33.6 (1C), 33.7 (1C), 33.8 (1C), 33.9 (1C), 114.1 (2C), 124.7 (2C), 129.0 (2C), 133.4 (2C), 137.4 (3C), 137.5 (1C), 139.2 (2C); ^{29}Si NMR ($CDCl_3$, 99.4 MHz) δ −1.0, −1.1; HRMS (ESI positive) m/z calcd for $C_{61}H_{102}Si_2$ + Na^+: 913.74122, found: 913.74123.

Synthesis of 1-(Tri-9-decenylsilyl)-4-(tri-8-nonenylsilyl)-naphthalene (11). Bissilylnaphthalene **11** was synthesized by the same procedure as **10**. In this case, the following reagents were used: 1-bromo-4-(tri-8-nonenylsilyl)naphthalene (**9**, 1.63 g, 2.79 mmol), THF (15 mL), n-BuLi solution (1.6 M in hexane, 2 mL, 1.0 equiv), and tri-9-decenylchlorosilane (**5**, 1.70 g, 3.43 mmol). Pure compound **11** (1.47 g, 1.50 mmol) was obtained as a colorless oil in 54% yield after GPC purification of the crude products. **11**: a colorless oil; ^{1}H NMR ($CDCl_3$, 500 MHz) δ 0.90−1.05 (m, 12H), 1.15−1.45 (m, 66H), 2.02 (q, J = 7.0 Hz, 12H), 4.92 (d, J = 10.0, 6H), 4.98 (d, J = 17.0 Hz, 6H), 5.78 (ddt, J = 17.0, 10.0, 7.0 Hz, 3H), 5.79 (ddt, J = 17.0, 10.0, 7.0 Hz, 3H), 7.46 (dd, J = 6.1, 3.4 Hz, 2H), 7.59 (s, 2H), 8.10 (dd, J = 6.1, 3.4 Hz, 2H); ^{13}C NMR ($CDCl_3$, 125 MHz) δ 13.6 (2C), 24.0 (2C), 29.0 (3C), 29.1 (2C), 29.2, 29.4, 33.7 (2C), 33.8 (2C), 114.1 (2C), 124.7 (2C), 129.0 (2C), 133.4 (2C), 137.4 (2C), 137.5 (2C), 139.2 (2C); ^{29}Si NMR ($CDCl_3$, 99.4 MHz) δ −1.1; HRMS (ESI positive) m/z calcd for $C_{67}H_{114}Si_2$ + Na^+: 997.83513, found: 997.83522.

Synthesis of Molecular Gyrotop C15 and Its Isomer C15i. To a solution of first-generation Grubbs' catalyst (0.05 g, 0.06 mmol) in dichloromethane (600 mL) was added 1-(tri-7-octenylsilyl)-4-(tri-8-nonenylsilyl)naphthalene (**10**) (960 mg, 1.07 mmol) in dichloromethane (200 mL) dropwise while stirring over 12 h, and the mixture was further stirred for 12 h. The volatile materials were removed *in vacuo*, and the metal catalyst was removed from the toluene-soluble fraction by flash column chromatography (silica gel, benzene). Hydrogen gas (3 atm) was then introduced in an autoclave to a solution of toluene (5 mL) and the reaction mixture in the presence of 10% Pd/C (0.03 g), and the mixture was allowed to stand for 72 h at 60 °C. After the excess H_2 gas was released, the mixture was filtered to remove the Pd/C. The volatile materials were removed *in vacuo*. The fractions containing **C15** and **C15i** were collected separately by GPC (chloroform), and the solvents were evaporated. Pure compound **C15** (120 mg, 0.15 mmol, 14% yield) was obtained as colorless crystals by recrystallization from THF/methanol (4:1). Pure compound **C15i** (251 mg, 0.30 mmol, 29% yield) was obtained without further purification. **C15**: colorless crystals; mp 100.1−101.3 °C; ^{1}H NMR ($CDCl_3$, 500 MHz) δ 0.80−1.21 (m, 36H), 1.22−1.60 (m, 54H), 7.46 (dd, J = 8.0, 4.0 Hz, 2H, 6- and 7-positions of Naphthalene), 7.62 (s, 2H, 2- and 3-positions of Naphthalene), 8.12 (dd, J = 8.0, 4.0 Hz, 2H, 5- and 8-positions of Naphthalene); ^{13}C NMR ($CDCl_3$, 125 MHz) δ 13.0 (2C), 15.3 (4C), 23.3(2C), 23.4 (4C), 27.4 (2C), 27.5 (2C), 27.6 (4C), 28.3 (6C), 28.5 (4C), 28.7 (2C), 28.8 (4C), 28.9 (1C), 29.3 (2C), 32.6 (4C), 32.7 (2C), 124.6 (2C, 6- and 7-positions of Naphthalene), 128.9 (2C, 5- and 8-positions of Naphthalene), 133.6 (2C, 2- and 3-positions of Naphthalene), 136.9 (2C, 1- and 4-positions of Naphthalene), 137.6 (2C, 4a- and 8a-positions of Naphthalene); ^{29}Si NMR ($CDCl_3$, 99.4 MHz) δ −0.5; HRMS (ESI positive) m/z calcd for $C_{55}H_{96}Si_2$ + Na^+: 835.69428, found: 835.69422. **C15i**: a colorless oil; ^{1}H NMR ($CDCl_3$, 500 MHz) δ 0.90−1.25 (m, 36H), 1.25−1.60 (m, 54H), 7.50 (dd, J = 6.0, 3.0 Hz, 2H), 7.64 (s, 2H), 8.15 (dd, J = 6.0, 3.0 Hz, 2H); ^{13}C NMR ($CDCl_3$, 125 MHz) δ 13.1, 13.3, 13.9, 14.0, 22.6, 23.3, 23.4, 26.4, 26.8, 26.9, 27.0, 27.1, 27.3, 27.6, 27.7, 28.0, 28.4, 28.5, 28.7, 27.0, 31.8, 32.7, 32.8, 32.8, 124.7, 129.0, 133.4, 137.3, 137.4; ^{29}Si NMR ($CDCl_3$, 99.4 MHz) δ −0.7 (1Si), −0.8 (1Si); HRMS (ESI positive) m/z calcd for $C_{55}H_{96}Si_2$ + Na^+: 835.69428 found:835.69430.

Synthesis of Molecular Gyrotop C17. Molecular gyrotop **C17** and its isomer **C17i** were synthesized from **11** (1.17 g, 1.20 mmol) by the same procedure as **C15**. Yields of the compounds were 13% for **C17** (135 mg, 0.15 mmol), and 28% for **C17i** (296 mg, 0.33 mmol). **C17**: colorless crystals; mp 135.6−137.8 °C; ^{1}H NMR ($CDCl_3$, 500 MHz) δ 0.90−1.05 (m, 12H), 1.05−1.50 (m, 90H), 7.49 (dd, J = 6.0, 3.5 Hz, 2H), 7.66 (s, 2H), 8.13 (dd, J = 6.0, 3.5 Hz, 2H); ^{13}C NMR ($CDCl_3$, 125 MHz) δ 14.1 (6C), 23.7 (6C), 28.4 (18C), 28.5 (6C), 29.0 (6C), 29.2 (3C), 33.3 (6C), 124.68, 129.68, 133.66, 137.29, 137.61; ^{29}Si NMR ($CDCl_3$, 99.4 MHz) δ −0.930; HRMS (ESI positive) m/z calcd for $C_{61}H_{108}Si_2$ + Na^+: 919.78818, found: 919.78821. **C17i**: a colorless oil; ^{1}H NMR ($CDCl_3$, 500 MHz) δ 0.95−1.60 (m, 102H), 7.48−7.58 (m, 2H), 7.67 (s, 2H), 8.12−8.23 (m, 2H); ^{13}C NMR ($CDCl_3$, 125 MHz) δ 13.3, 13.4, 14.2, 23.3, 23.6, 23.8, 27.1, 27.4, 27.6, 27.7, 28.0, 28.1, 28.2, 28.3, 28.5, 28.8, 28.9, 29.0, 32.7, 33.3, 33.5, 124.7, 129.0, 133.5, 137.4, 137.5; ^{29}Si NMR ($CDCl_3$, 99.4 MHz) δ −0.9 (2Si); HRMS (ESI positive) m/z calcd for $C_{61}H_{108}Si_2$ + Na^+: 919.78818, found: 919.78819.

Synthesis of Molecular Gyrotop C14. Molecular gyrotop **C14**[4d] and its isomer **C14i** were synthesized from **6** (589 mg, 0.77 mmol) by the same procedure as **C15**. Yields of the compounds were 29% for **C14**[4d] (164 mg, 0.22 mmol), and 27% for **C14i** (154 mg, 0.21 mmol). **C14i**: a colorless oil; ^{1}H NMR ($CDCl_3$, 400 MHz) δ 0.80−1.21 (m, 36H), 1.22−1.60 (m, 48H), 7.46 (dd, J = 8.0, 4.0 Hz, 2H), 7.62 (s, 2H), 8.12 (dd, J = 8.0, 4.0 Hz, 2H); ^{13}C NMR ($CDCl_3$, 100 MHz) δ 13.1 (4C), 13.8 (2C), 22.6 (4C), 23.2 (2C), 26.3 (4C), 26.8 (4C), 26.9 (4C), 27.0 (4C), 27.4 (2C), 27.6 (2C), 28.1 (2C), 28.3 (2C), 31.8 (4C), 32.5 (2C), 124.7 (2C), 128.9 (2C), 133.4 (2C), 137.3 (2C), 137.6 (2C); ^{29}Si NMR ($CDCl_3$, 79.5 MHz) δ −0.5; Anal. Calcd for $C_{52}H_{90}Si_2$: C, 80.96; H, 11.76. Found: C, 80.97; H, 11.85.

Synthesis of Molecular Gyrotop C16. Molecular gyrotop **C16**[4d] and its isomer **C16i** were synthesized from **7** (1.00 g, 1.07 mmol) by the same procedure as **C15**. Yields of the compounds were 7% for **C16**[4d] (63 mg, 0.073 mmol), and 32% for **C16i** (288 mg, 0.34 mmol). **C16i**: a colorless oil; ^{1}H NMR ($CDCl_3$, 400 MHz) δ 0.95−1.30, 1.30−1.68, 7.52 (dd, J = 8.0, 4.3 Hz, 2H), 7.68 (s, 2H), 8.18 (dd, J = 8.0, 4.3 Hz, 2H); ^{13}C NMR ($CDCl_3$, 100 MHz) δ 13.1, 14.1, 23.3, 23.9, 27.2, 27.6, 27.7, 28.1, 28.3, 28.4, 28.7, 32.8, 33.3, 124.7, 129.0, 133.5, 137.4; ^{29}Si NMR ($CDCl_3$, 79.5 MHz) δ −0.7; Anal. Calcd for $C_{58}H_{102}Si_2$: C, 81.42; H, 12.02. Found: C, 81.61; H, 11.80.

Synthesis of Molecular Gyrotop C18. Molecular gyrotop **C18**[4d] and its isomer **C18i** were synthesized from **8** (555 g, 0.596 mmol) by the same procedure as **C15**. Yields of the compounds were 18% for **C18**[4d] (101 mg, 0.11 mmol), and 15% for **C18i** (86 mg, 0.092 mmol). **C18i**: a colorless oil; ^{1}H NMR ($CDCl_3$, 400 MHz) δ 0.95−1.50 (m, 108H), 7.49 (dd, J = 8.0, 4.3 Hz, 2H), 7.64 (s, 2H), 8.14 (dd, J = 8.0, 4.3 Hz, 2H); ^{13}C NMR ($CDCl_3$, 100 MHz) δ 13.3, 14.3, 23.6, 24.0, 27.4, 27.6, 28.1, 28.2, 28.3, 28.4, 28.5, 28.7, 28.8, 33.3, 33.6, 124.7, 129.1, 133.4, 137.4, 137.5; ^{29}Si NMR ($CDCl_3$, 79.5 MHz) δ −0.879; Anal. Calcd for $C_{64}H_{114}Si_2$: C, 81.80; H, 12.23. Found: C, 81.68; H, 12.47.

X-ray Crystallographic Analyses of Two Molecular Gyrotops. The diffraction data of molecular gyrotops **C15** and **C17** were collected using graphite-monochromatized Mo Kα radiation (λ = 0.71069 Å). Crystallographic data for **C15** (120 K): monoclinic, $P2_1/c$, a = 22.779(6) Å, b = 12.654(3) Å, c = 18.025(5) Å, β = 90.008(4)°, V = 5195(2) Å3, $R1$ = 0.1058 ($I > 2\sigma I$), $wR2$ = 0.2935 (all data). Crystallographic data for **C17** (90 K): triclinic, $P\bar{1}$, a = 13.028(9) Å, b

DOI: 10.1021/acs.joc.5b01489
J. Org. Chem. 2015, 80, 9959−9966

= 18.089(13) Å, c = 25.708(18) Å, α = 74.702(12)°, β = 83.371(15)°, γ = 89.177(15)°, V = 5804(7) Å^3, $R1$ = 0.1874 ($I > 2\sigma I$), $wR2$ = 0.5740 (all data). The crystallographic data were deposited at the Cambridge Crystallographic Database Centre (CCDC-1407304 for **C15**, and CCDC-1407258 for **C17**).

■ ASSOCIATED CONTENT

Supporting Information

The Supporting Information is available free of charge on the ACS Publications website at DOI: 10.1021/acs.joc.5b01489.

Copies of NMR spectra for all new compounds (**9**, **10**, **11**, **C14i**, **C15**, **C15i**, **C16i**, **C17**, **C17i**, and **C18i**). Details of temperature-dependent ^{13}C NMR studies of **C14**, **C15**, **C17**, and **C18**. Details of fluorescence lifetime measurements of silylnaphthalenes (PDF)

Crystallographic data for **C15** (CIF)

Crystallographic data for **C17** (CIF)

■ AUTHOR INFORMATION

Corresponding Author

*E-mail: wsetaka@tmu.ac.jp.

Notes

The authors declare no competing financial interest.

■ ACKNOWLEDGMENTS

We thank Mr. H. Monma (Tohoku University) for the HRMS measurements of the new compounds. This work was supported by a JSPS Grant-in-Aid for Scientific Research (B) (W.S. and K.Y., no. 25288042) and Scientific Research on Innovation Areas "Stimuli-responsive Chemical Species" (W.S., no. 15H00955).

■ REFERENCES

(1) (a) Vogelsberg, C. S.; Garcia-Garibay, M. A. *Chem. Soc. Rev.* **2012**, *41*, 1892. (b) Karim, A. R.; Linden, A.; Baldridge, K. K.; Siegel, J. S. *Chem. Sci.* **2010**, *1*, 102. (c) Blanzani, V.; Credi, A.; Venturi, M. *Molecular Devices and Machines*, 2nd ed.; Wiley-VCH: Weinheim, 2008. (d) Kay, E. R.; Leigh, D. A.; Zerbetto, F. *Angew. Chem., Int. Ed.* **2007**, *46*, 72. (e) Browne, W. R.; Feringa, B. L. *Nat. Nanotechnol.* **2006**, *1*, 25. (f) Kelly, T. R., Ed. *Molecular Machines*; Topics in Current Chemistry; Springer: Hidelberg, 2005; Vol. *262*. (g) Kottas, G. S.; Clarke, L. I.; Horinek, D.; Michl, J. *Chem. Rev.* **2005**, *105*, 1281. (h) Garcia-Garibay, M. A. *Proc. Natl. Acad. Sci. U.S.A.* **2005**, *102*, 10771. (i) Balzani, V.; Credi, A.; Raymo, F. M.; Stoddart, J. F. *Angew. Chem., Int. Ed.* **2000**, *39*, 3348.

(2) (a) Commins, P.; Garcia-Garibay, M. A. *J. Org. Chem.* **2014**, *79*, 1611. (b) Commins, P.; Nuñez, J. E.; Garcia-Garibay, M. A. *J. Org. Chem.* **2011**, *76*, 8355. (c) Nuñez, J. E.; Natarajan, A.; Khan, S. I.; Garcia-Garibay, M. A. *Org. Lett.* **2007**, *9*, 3559.

(3) (a) Nawara-Hultzsch, A. J.; Stollenz, M.; Barbasiewicz, M.; Szafert, S.; Lis, T.; Hampel, F.; Bhuvanesh, N.; Gladysz, J. A. *Chem.—Eur. J.* **2014**, *20*, 4617. (b) Zeits, P. D.; Rachiero, G. P.; Hampel, F.; Reibenspies, J. H.; Gladysz, J. A. *Organometallics* **2012**, *31*, 2854. (c) Skopek, K.; Gladysz, J. A. *J. Organomet. Chem.* **2008**, *693*, 857. (d) Skopek, K.; Barbasiewicz, M.; Hampel, F.; Gladysz, J. A. *Inorg. Chem.* **2008**, *47*, 3474. (e) Han, J.; Deng, C.; Fang, R.; Zhao, D.; Wang, L.; Gladysz, J. A. *Organometallics* **2010**, *29*, 3231. (f) Hess, G. D.; Hampel, F.; Gladysz, J. A. *Organometallics* **2007**, *26*, 5129. (g) Wang, L.; Shima, T.; Hampel, F.; Gladysz, J. A. *Chem. Commun.* **2006**, 4075. (h) Wang, L.; Hampel, F.; Gladysz, J. A. *Angew. Chem., Int. Ed.* **2006**, *45*, 4372. (i) Nawara, A. J.; Shima, T.; Hampel, F.; Gladysz, J. A. *J. Am. Chem. Soc.* **2006**, *128*, 4962. (j) Shima, T.; Hampel, F.; Gladysz, J. A. *Angew. Chem., Int. Ed.* **2004**, *43*, 5537.

(4) (a) Setaka, W.; Inoue, K.; Higa, S.; Yoshigai, S.; Kono, H.; Yamaguchi, K. *J. Org. Chem.* **2014**, *79*, 8288. (b) Setaka, W.; Higa, S.; Yamaguchi, K. *Org. Biomol. Chem.* **2014**, *12*, 3354. (c) Setaka, W.; Yamaguchi, K. *J. Am. Chem. Soc.* **2013**, *135*, 14560. (d) Setaka, W.; Koyama, A.; Yamaguchi, K. *Org. Lett.* **2013**, *15*, 5092. (e) Setaka, W.; Yamaguchi, K. *Proc. Natl. Acad. Sci. U.S.A.* **2012**, *109*, 9271. (f) Setaka, W.; Yamaguchi, K. *J. Am. Chem. Soc.* **2012**, *134*, 12458. (g) Shionari, H.; Inagaki, Y.; Yamaguchi, K.; Setaka, W. *Org. Biomol. Chem.*, in press (DOI:**2015**10.1039/C5OB01644D).

(5) (a) Setaka, W.; Ohmizu, S.; Kira, M. *Chem. Commun.* **2014**, *50*, 1098. (b) Marahatta, A. B.; Kanno, M.; Hoki, K.; Setaka, W.; Irle, S.; Kono, H. *J. Phys. Chem. C* **2012**, *116*, 24845. (c) Setaka, W.; Ohmizu, S.; Kira, M. *Chem. Lett.* **2010**, *39*, 468. (d) Setaka, W.; Ohmizu, S.; Kabuto, C.; Kira, M. *Chem. Lett.* **2007**, *36*, 1076.

(6) (a) Dominguez, Z.; Dang, H.; Strouse, M. J.; Garcia-Garibay, M. A. *J. Am. Chem. Soc.* **2002**, *124*, 2398. (b) Godinez, C. E.; Zepeda, G.; Garcia-Garibay, M. A. *J. Am. Chem. Soc.* **2002**, *124*, 4701. (c) Dominguez, Z.; Dang, H.; Strouse, M. J.; Garcia-Garibay, M. A. *J. Am. Chem. Soc.* **2002**, *124*, 7719. (d) Dominguez, Z.; Khuong, T.-A. V.; Dang, H.; Sanrame, C. N.; Nuñez, J. E.; Garcia-Garibay, M. A. *J. Am. Chem. Soc.* **2003**, *125*, 8827. (e) Horansky, R. D.; Clarke, L. I.; Winston, E. B.; Price, J. C.; Karlen, S. D.; Jarowski, P. D.; Santillan, R.; Garcia-Garibay, M. A. *Phys. Rev. B: Condens. Matter Mater. Phys.* **2006**, *74*, 054306. (f) Horansky, R. D.; Clarke, L. I.; Price, J. C.; Khuong, T.-A. V.; Jarowski, P. D.; Garcia-Garibay, M. A. *Phys. Rev. B: Condens. Matter Mater. Phys.* **2005**, *72*, 014302. (g) Vogelsberg, C. S.; Bracco, S.; Beretta, M.; Comotti, A.; Sozzani, P.; Garcia-Garibay, M. A. *J. Phys. Chem. B* **2012**, *116*, 1623. (h) Czajkowska-Szczykowska, D.; Rodríguez-Molina, B.; Magaña-Vergara, N. E.; Santillan, R.; Morzycki, J. W.; Garcia-Garibay, M. A. *J. Org. Chem.* **2012**, *77*, 9970. (i) Rodríguez-Molina, B.; Pérez-Estrada, S.; Garcia-Garibay, M. A. *J. Am. Chem. Soc.* **2013**, *135*, 10388. (j) Rodríguez-Molina, B.; Ochoa, M. E.; Romero, M.; Khan, S. I.; Farfán, N.; Santillan, R.; Garcia-Garibay, M. A. *Cryst. Growth Des.* **2013**, *13*, 5107. (k) Torres-Huerta, A.; Rodríguez-Molina, B.; Höpfl, H.; Garcia-Garibay, M. A. *Organometallics* **2014**, *33*, 354. (l) Jiang, X.; Rodríguez-Molina, B.; Nazarian, N.; Garcia-Garibay, M. A. *J. Am. Chem. Soc.* **2014**, *136*, 8871.

(7) (a) Bastien, G.; Lemouchi, C.; Wzietek, P.; Simonov, S.; Zorina, L.; Rodríguez-Fortea, A.; Canadell, E.; Batail, P. *Z. Anorg. Allg. Chem.* **2014**, *640*, 1127. (b) Lemouchi, C.; Yamamoto, H. M.; Kato, R.; Simonov, S.; Zorina, L.; Rodríguez-Fortea, A.; Canadell, E.; Wzietek, P.; Iliopoulos, K.; Gindre, D.; Chrysos, M.; Batail, P. *Cryst. Growth Des.* **2014**, *14*, 3375. (c) Comotti, A.; Bracco, S.; Yamamoto, A.; Beretta, M.; Hirukawa, T.; Tohnai, N.; Miyata, M.; Sozzani, P. *J. Am. Chem. Soc.* **2014**, *136*, 618. (d) Lemouchi, C.; Iliopoulos, K.; Zorina, L.; Simonov, S.; Wzietek, P.; Cauchy, T.; Rodríguez-Fortea, A.; Canadell, E.; Kaleta, J.; Michl, J.; Gindre, D.; Chrysos, M.; Batail, P. *J. Am. Chem. Soc.* **2013**, *135*, 9366.

(8) (a) Claridge, T. D. W. *High Resolution NMR Techniques in Organic Chemistry*; Pergamon: Oxford, U.K., 1999; Section 8.7.4. (b) Ernst, R. R.; Bodenhausen, G.; Wokaun, A. *Principles of Nuclear Magnetic Resonance in One and Two Dimensions*; Clarendon: Oxford, U.K., 1987. (c) Perrin, C. L.; Dwyer, T. J. *Chem. Rev.* **1990**, *90*, 935.

(9) (a) Jeener, J.; Meier, B. H.; Bachmann, P.; Ernst, R. R. *J. Chem. Phys.* **1979**, *71*, 4546. (b) Gridnev, I. D.; Tok, O. L.; Gridneva, N. A.; Bubnov, Y. N.; Schreiner, P. R. *J. Am. Chem. Soc.* **1998**, *120*, 1034.

(10) (a) Herndon, J. W. *Coord. Chem. Rev.* **2014**, *272*, 48. (b) Fürstner, A. *Science* **2013**, *341*, 1229713. (c) Grubbs, R. H., Ed. *Handbook of Metathesis*; Wiley-VCH: Weinheim, 2003; Vols. *1*−*3*. (d) Schrock, R. R. *Angew. Chem., Int. Ed.* **2006**, *45*, 3748. (e) Grubbs, R. H. *Angew. Chem., Int. Ed.* **2006**, *45*, 3760. (f) Vougioukalakis, G. C.; Grubbs, R. H. *Chem. Rev.* **2010**, *110*, 1746.

(11) Cobas, J. C.; Martin-Pastor, M. *EXSYCalc Ver 1.0*; Mestrelab Research S.L.: A Coruña, Spain, 2007.

(12) (a) Maeda, H.; Maeda, T.; Mizuno, K. *Molecules* **2012**, *17*, 5108. (b) Shizuka, H.; Obuchi, H.; Ishikawa, M.; Kumada, M. *J. Chem. Soc., Faraday Trans. 1* **1984**, *80*, 383. (c) Ishikawa, M.; Oda, M.; Miyoshi, N.; Fábry, L.; Kumada, M.; Yamabe, T.; Akagi, K.; Fukui, K. *J. Am. Chem. Soc.* **1979**, *101*, 4612. (d) Pitt, C. G.; Carey, R. N.; Toren, E. C., Jr. *J. Am. Chem. Soc.* **1972**, *94*, 3806.

(13) Weber, G.; Teale, F. W. J. *Trans. Faraday Soc.* **1957**, *53*, 646.

DOI: 10.1021/acs.joc.5b01489
J. Org. Chem. 2015, 80, 9959−9966